

ARTICLE

Received 2 Aug 2010 | Accepted 9 Sep 2010 | Published 19 Oct 2010 | Corrected online 22 Oct 2010

DOI: 10.1038/ncomms1088

Effects of electronegative substitution on the optical and electronic properties of acenes and diazaacenes

Anthony Lucas Appleton¹, Scott M. Brombosz¹, Stephen Barlow¹, John S. Sears¹, Jean-Luc Bredas¹, Seth R. Marder¹ & Uwe H.F. Bunz^{1,†}

Large acenes, particularly pentacenes, are important in organic electronics applications such as thin-film transistors. Derivatives where CH units are substituted by sp^2 nitrogen atoms are rare but of potential interest as charge-transport materials. In this article, we show that pyrazine units embedded in tetracenes and pentacenes allow for additional electronegative substituents to induce unexpected redshifts in the optical transitions of diazaacenes. The presence of the pyrazine group is critical for this effect. The decrease in transition energy in the halogenated diazaacenes is due to a disproportionate lack of stabilization of the HOMO on halogen substitution. The effect results from the unsymmetrical distribution of the HOMO, which shows decreased orbital coefficients on the ring bearing chlorine substituents. The more strongly electron-accepting cyano group is predicted to shift the transitions of diazaacenes even further to the red. Electronegative substitution impacts the electronic properties of diazaacenes to a much greater degree than expected.

¹ School of Chemistry and Biochemistry, Georgia Institute of Technology, 901 Atlantic Drive, Atlanta, Georgia 30332, USA. [†]Present address: Organisch Chemisches Institut, Ruprecht-Karls-Universität, Im Neuenheimer Feld 270, Heidelberg 69120, Germany. Correspondence and requests for materials should be addressed to U.H.F.B. (email: bunz@oci.uni-heidelberg.de).

The larger acene cores provide a particularly attractive framework for the design of molecules with tunable properties that can be useful for organic electronic applications. Pentacenes such as **1**¹ or **5**, but also **2** (first prepared by Hinsberg²), are of major interest as hole-transport materials in thin-film transistors³ and have high charge-carrier mobilities, because of their favourable solid-state packing and small reorganization energies^{4–6}; pentacene is also a component of reference for systems in the development of small-molecule organic solar cells⁷. Although Houk suggested that larger *N*-heteroacenes could behave as electron-transport materials when suitably substituted⁸, to date acenes have generally functioned as hole-transport materials. Only a few acenes have shown appreciable electron mobilities^{9–12}. To realize the full potential of acenes and heteroacenes, it is essential to expand the scope of materials available. Figure 1a shows recent and historical members in the series of pentacenes^{13,14}. Chlorinated pentacenes such as **6** were processed into ambipolar transistors. Chlorination lowers both HOMO and LUMO, but with the former effect insufficient to preclude hole injection, whereas the latter effect facilitates electron injection; however, the optical gap does not change to any appreciable extent¹⁵. The tetrachloro substitution only led to a slight shift in the absorption maximum going from 643 nm for **5**¹⁶ to 654 nm for **6** in solution, suggesting that chlorine substitution had comparable impact on both the ground and first excited states^{17–19}. Lowering the absorption

energies can be useful in the context of organic solar cells when looking for acene derivatives showing absorption into the near-infrared, as observed in Anthony's hexacenes and heptacenes^{20,21}.

We report here the simple synthesis of novel heteroacenes, *viz.* diazapentacene **15a**, the halogenated diazatetracene **11b** and the tetrahalodiazapentacenes **15b,c** (Fig. 1b). Electronegative substitution, that is, transforming **11a**→**11b** and **15a**→**15b,c**, causes surprising bathochromic shifts in absorption, in addition to the improved reducibility anticipated through stabilization of the LUMOs by electronegative substitution²².

Results

Synthesis. Condensation of **9** (Fig. 2a) with **10b** gave tetrachloro-diazatetracene **11b** smoothly and in good yields. For comparison purposes we also re-synthesized **11a**²³. The diamine **13** (Fig. 2b) was obtained by LiAlH₄ reduction of **12** (ref. 24) and reacted with **10a–c** to furnish the *N,N*-dihydrodiazapentacenes **14a–c** in moderate yields; **14a–c** were oxidized by manganese dioxide to give **15a–c** after chromatography as green-black, environmentally stable crystalline materials almost quantitatively.

Optical spectra and cyclic voltammetry. Figure 3a shows the long-wavelength features of the UV-Vis spectra of a selection of the diazatetracenes and diazapentacenes and, as a comparison, the

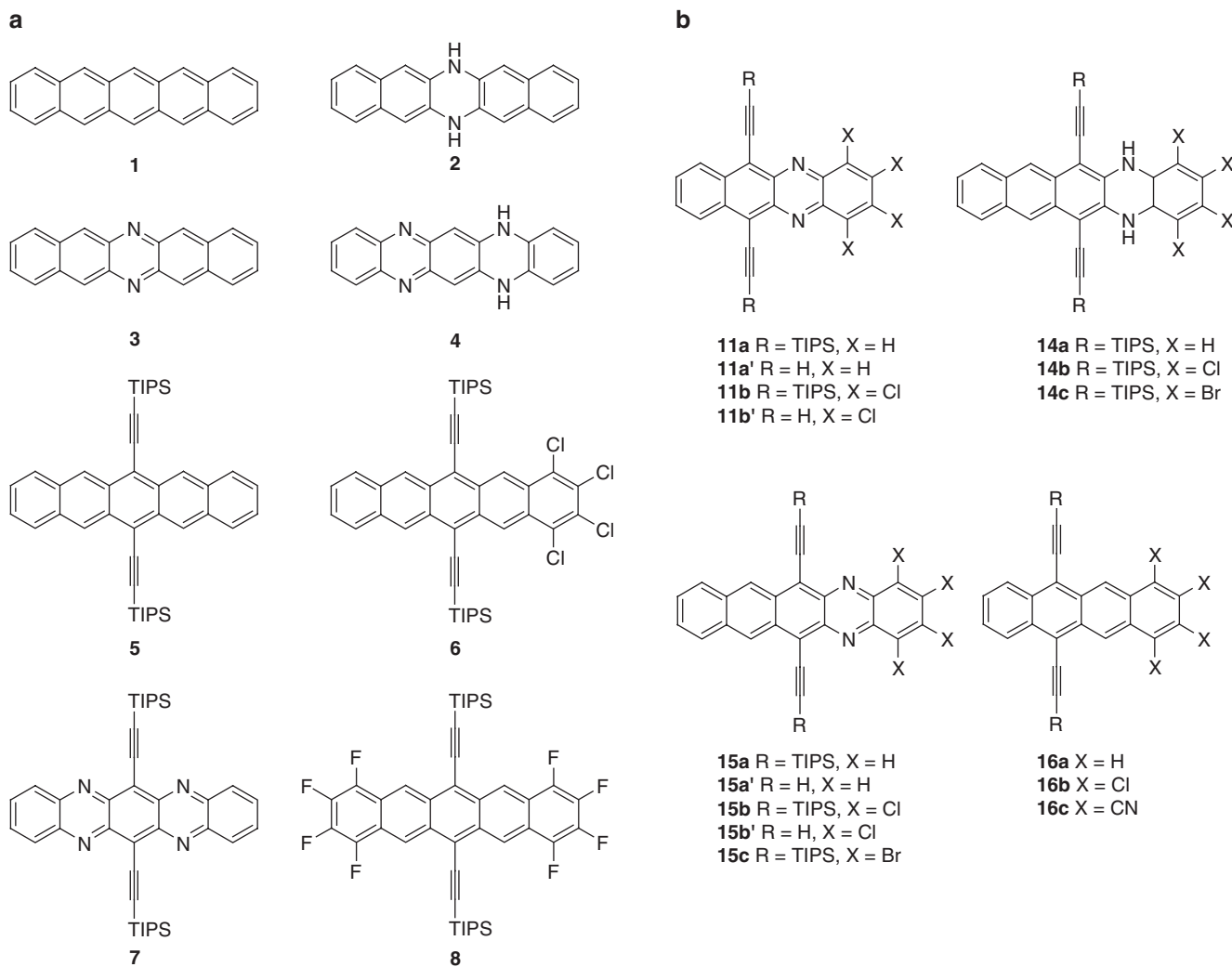


Figure 1 | Pentacene compounds of current and historical interest and the target compounds produced herein. (a) Compounds prepared by (1) Clar,¹ (2) Hinsberg², (3) Zimmermann²², (4) Fischer³⁰, (5) Anthony⁵, (6) Bao¹⁵, (7) Bunz¹³, (8) Bao¹⁰. (b) Compounds prepared in this paper (**11a,b**, **14a–c**, **15a–c**) and calculated model compounds (**11a',b', 15a',b', 16a–c**).

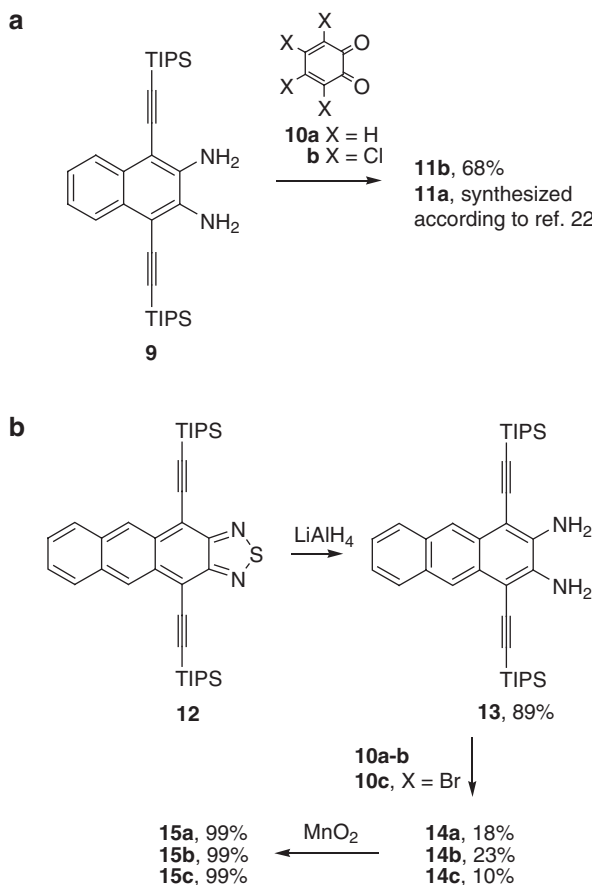


Figure 2 | Synthesis of diazatetracene 11b and diazapentacenes 15. (a) The condensation of the diamine **9** with the *ortho*-quinones **10a** and **10b** furnished the diazaacenes **11a** and **11b** in excellent yield. (b) On reacting **13** with **10**, the NH intermediates **14a-c** are isolated and oxidized efficiently to **15a-c**, respectively, by manganese dioxide.

UV-Vis spectrum of the tetraazapentacene **7** (ref. 13). Figure 3b shows a photograph of solutions of these materials. The absorption spectrum of **11b** (in hexane) shows a λ_{max} of 617 nm, whereas **11a**, the parent, shows a λ_{max} of 571 nm; that is, the tetrachloro substitution leads to a redshift of 1,306 cm⁻¹ or 0.16 eV, whereas, in comparison, tetrachloropentacene **6** shows an absorption maximum only 0.032 eV lower in energy than that of the parent compound **5**, according to reported UV-Vis spectra (ref. 24).

The UV-Vis spectra of the NH compounds **14a-c** are similar to each other, but show a slight hypsochromic, rather than bathochromic, shift when going from the parent to the halogenated species (**14a**: $\lambda_{\text{max}} = 493$ nm; **14b**: $\lambda_{\text{max}} = 479$ nm; **14c**: $\lambda_{\text{max}} = 482$ nm (Supplementary Figs S1 and S2), whereas **15a-c** again show bathochromically shifted spectral features. Table 1 shows parameters characterizing the absorption spectra, the results of the cyclic voltammetry measurements (Supplementary Table S1) and of quantum chemical calculations using density functional (DFT) and time-dependent density functional theory (TD-DFT) of derivatives of **11** and **15** (Supplementary Table S2).

The diazapentacene **15a** has a molar extinction coefficient ($\epsilon = 1.9 \times 10^4$; Table 1) that is close to that of **5** ($\epsilon = 2.0 \times 10^4$). The introduction of halogen substituents in **11** and **15** leads to some (**11**→**11b**, **15a**→**15b**) decreases in the extinction coefficients. Also the redshifts observed in the solution absorption persist in the solid state and are approximately 800–900 cm⁻¹ when going from solution into the solid state for the diazapentacenes (Table 1). Both of the tetracenes (**11a** and **11b**), as well as diazapentacene **15a**, are

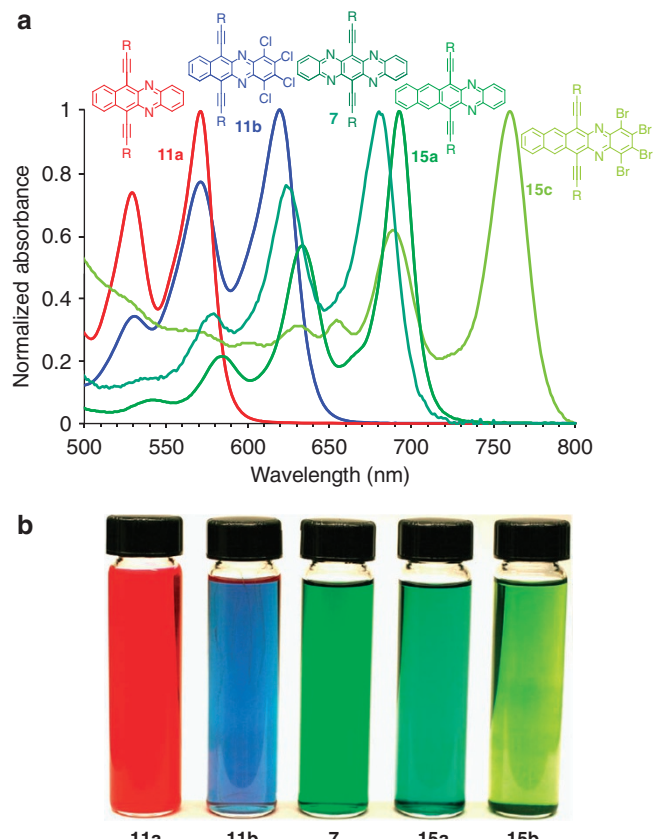


Figure 3 | UV-Vis spectra of selected heteroacenes. (a) Long-wavelength normalized UV-Vis spectra in hexane; R = TIPS in all cases. (b) Photograph of solutions of heteroacenes in hexane. The combined effects of annulation and halogenation lead to a shift of absorption from 571 to 758 nm. The spectrum of **15b** is almost superimposable onto that of **15c**. The halo-substitution in both tetracenes and in pentacenes leads to significant redshifts in absorption. Chlorine and bromine substituents are equally effective. The UV-Vis spectrum of **7** was taken from Miao et al.¹³

fluorescent, the diazatetracenes more so than the diazapentacenes, whereas the halogenated diazapentacenes are non-fluorescent.

Quantum chemical calculations. To further explore the effect of electronegative substitution in heteroacenes, we performed DFT and TD-DFT calculations on model compounds with structures derived from **11** and **16**. Table 1 shows the TD-DFT values of the vertical transition energies (S_1^{vert}) for the lowest-lying singlet excited states of model compounds **11a'**, **11b'**, **15a'** and **15b'**. The calculations reproduce the trends observed in the experimental data of **11a,b** and **15a,b**; TD-DFT calculations for the tetracenes **16a** and **16b** predict only a very small redshift in absorption as a result of chlorination, which is also consistent with experimental data for the corresponding homolog pentacenes, **5** and **6**.

Figure 4a shows the frontier molecular orbitals (energy in eV) of **11a'**/**11b'** and **16a**/**16b**. In both pairs, stabilization of the LUMOs results when attaching four chlorine substituents. The stabilization is 0.43 eV in both **11b'** and **16b**. More importantly, on going from **11a'** to **11b'** the HOMO is only stabilized by 0.31 eV, whereas in the case of **16a**/**16b** the HOMO stabilization is 0.40 eV, very similar to that observed for the LUMO. On the basis of computational results, the contribution (sum of the squared orbital coefficients) from rings 3 and 4 is about three times as large in **16a** as in the heteroacene **11a'**. To investigate the influence of even stronger acceptors, we performed quantum chemical calculations on model

Table 1 | Absorption and emission maxima and electrochemistry of the investigated heteroacenes.

| Acene | 11a | 11b | 11c | 15a | 15b | 15c | 16a | 16b | 16c |
|---|----------|-----------|-------|-----------|-----------------|-----------------|-------|-------|-------|
| X= | H | Cl | CN | H | Cl | Br | H | Cl | CN |
| λ_{max} abs (nm) | 571 | 617 | — | 692 | 756 | 759 | — | — | — |
| ϵ_{max} ($10^3 \text{ M}^{-1} \text{ cm}^{-1}$) | 22.7 | 17.3 | — | 19.1 | 12.9 | 10.2 | — | — | — |
| λ_{max} abs,ss (nm) [cm^{-1}]* | 573 [79] | 636 [484] | — | 737 [892] | 806 [821] | ND | — | — | — |
| λ_{max} emission (nm) | 582 | 635 | — | 713 | Non-fluorescent | Non-fluorescent | — | — | — |
| Quantum yield Φ | 0.09 | 0.02 | — | < 0.01 | — | — | — | — | — |
| $E_{1/2}^{0/-} (\text{V})^{\ddagger}$ | -1.19 | -0.92 | — | -1.05 | -0.79 | -0.79 | — | — | — |
| $E_{1/2}^{+/-} (\text{V})^{\ddagger}$ | +0.99 | +1.11 | — | +0.68 | +0.83 | +0.80 | — | — | — |
| Elchem. gap (V) | 2.18 | 2.03 | — | 1.73 | 1.62 | 1.59 | — | — | — |
| Opt. gap (eV)† | 2.17 | 2.01 | — | 1.79 | 1.64 | 1.63 | — | — | — |
| $S_1^{\text{vert}\S}$ | 2.07 | 1.91 | 1.38 | 1.58 | 1.44 | ND | 2.16 | 2.13 | 1.61 |
| calcd. HOMO-LUMO gap (eV)¶ | 2.37 | 2.25 | 1.81 | 1.87 | 1.77 | ND | 2.41 | 2.39 | 2.00 |
| HOMO (eV) | -5.72 | -6.03 | -6.66 | -5.37 | -5.66 | ND | -5.28 | -5.68 | -6.38 |
| LUMO (eV) | -3.35 | -3.78 | -4.84 | -3.50 | -3.89 | ND | -2.87 | -3.30 | -4.38 |

*Solid state absorption in thin films. The values in square brackets are the shifts observed when going from solution into thin solid films.

†From absorption maxima.

‡In a 1:1 (v/v) mixture of a 0.1M acetonitrile solution of Bu_4NPF_6 and toluene, vs $\text{FeCp}_2^{+/-}$.

§STD-DFT calculations at the B3LYP/6-311+G* level. The transitions are all one-electron transitions with a >80% HOMO-LUMO contribution.

¶The desilylated model compounds **11a'**, **11b'**, **15a'** and **15b'** were used for the calculations to reduce the computation time. DFT B3LYP/6-311+G*//6-311+G* method was used.

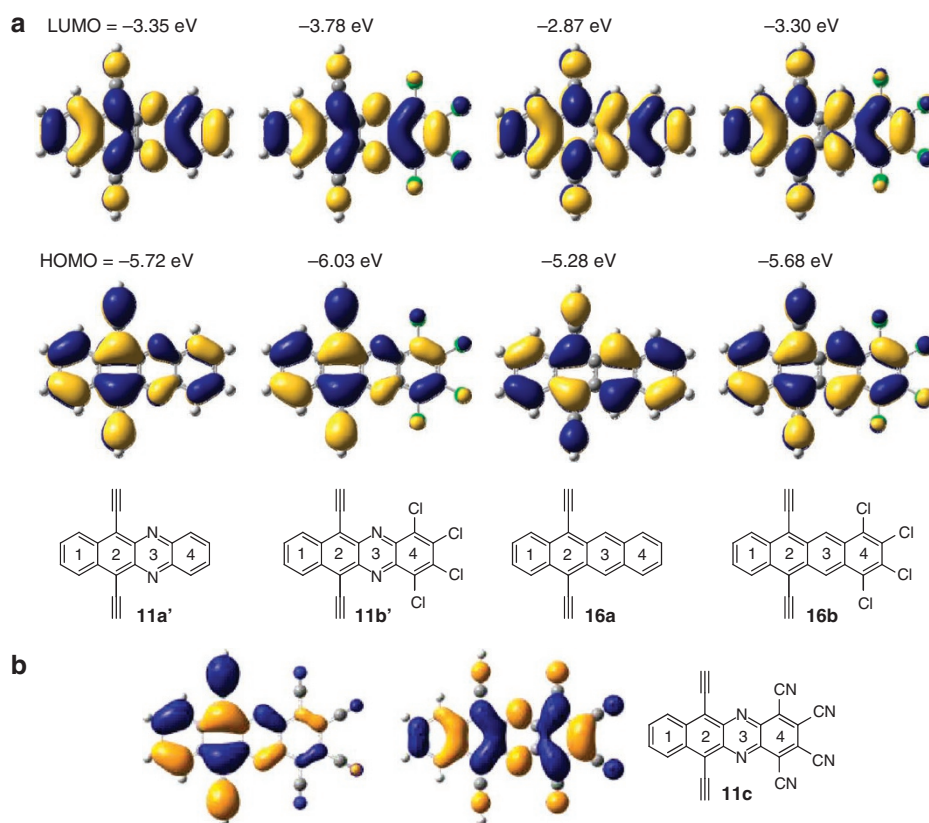


Figure 4 | Frontier molecular orbitals of acene derivatives. HOMO, middle; LUMO, top. The middle bottom row shows the structural formulae and numbering of the rings. (a) The LUMOs of the four compounds are very similar to each other. Both the LUMOs of **11b'** and **16b** experience a stabilization of 0.43 eV through the chlorine substitution. The HOMOs of **11a'**/**11b'** and **16a**/**16b** resemble each other qualitatively but are pair wise (**11/16**) different. The differences are pronounced in the rings 3 and 4 as particularly in the HOMO of **11a'** the orbital coefficients (see SI) on the rings 3 and 4 are small; as a consequence the chlorine substituents are less effective in stabilizing the HOMO (going from **11a'** to **11b'**), mirroring the optical behaviour seen in compound **11b**. (b) Frontier molecular orbitals (HOMO 6.30 eV, left; LUMO 4.49 eV, right; gap = 1.81 eV) of tetracyanodiazacene **11c**. Calculated by DFT using B3LYP/6-311+G* basis sets. Compared to **11a'** calculated on the same level of theory, the optical band gap (S_0 - S_1 transition) shrinks from 2.07 to 1.38 eV.

11c (Fig. 4b). The HOMO of **11c** is predominantly localized on rings 1 and 2, whereas the LUMO is extended over all four rings; as a result, the calculated optical gap shrinks from 2.07 eV in **11a** to 1.38 eV in **11c**.

Discussion

Larger functionalized heteroacenes are virtually unknown. The synthesis of the diazatetracenes **11a,b** proceeds smoothly by simple condensation of a diamine with an *ortho*-quinone. In the case of the diazapentacenes

15a–c, the condensation first leads to **14a–c**, which are then oxidized into **15a–c**. It has been noted that the formally anti-aromatic **14a–c**^{1,25} are stabilized by the interplay of energetically advantageous enamine groups and the presence of two Clar sextets instead of one for the heteroacenes **15a–c**. In the diazatetracenes **11**, this delicate energetic balance is such that the overall aromaticity drives the formation of **11**, and the significantly more anti-aromatic NH compounds are not observed as already shown by Hinsberg for the parent diazatetracene in 1901 (refs 2, 25). However, oxidation of **14** into **15** is facile and quantitative.

The most interesting and important discovery of this contribution is the significant redshifts that are observed when attaching halogen substituents to diazaacenes. The spectral redshift observed when going from **11a** to **11b** and from **15a** to **15b** or **15c** is evident in Figure 3. By change of substituent and size of the acene framework, an absorption range from 561 to 758 nm can be ‘tuned in’ in **11** and **15**. The expected acene-type vibronic fine structure is observed for all of the compounds and, although the extinction coefficient decreases on addition of the electronegative substituents, the effect is not dramatic, suggesting that these materials could be useful absorbers. Electronegative substitution on π systems can lead to either blue- or redshifted or almost unchanged absorption spectra; chlorination, for example, induces bathochromic shifts in 9,10-dichloroanthracene¹⁷ and in some chlorinated nitro-aminodiazobenzene derivatives of disperse red¹⁸. Such electronegativity effects occur if either the HOMO or the LUMO is particularly stabilized or not; they are especially pronounced in molecules with disjoint orbital structures, where HOMO and LUMO are localized on different parts of the molecule. However, the contrast of the pairs **11a**–**b**/**15a**–**b** and **5**/**6** was unusually large and unanticipated. Also surprisingly, the effect of bromine and chlorine substituents on the optical features of the diazaacenes is almost identical. This is however consistent with the similar inductive and mesomeric properties of these two halogens (Br: $F = +0.45$, $R = -0.22$; Cl: $F = +0.42$, $R = -0.19$; F =field effect parameter, R =resonance parameter) that is, both substituents function as moderately inductive (σ) electron-withdrawing groups and as weak π -donors, as indicated by the Swain–Lupton parameters quantifying these two effects²⁶.

The calculations indicate in all cases that the transitions are predominantly HOMO-to-LUMO in character. The trends in the electrochemical gaps between the half-wave potentials corresponding to molecular oxidation and reduction closely follow those in the experimental and TD-DFT optical transition energies and the DFT HOMO-LUMO gaps (Table 1). The very close correspondence between the values of the experimental optical and electrochemical gaps (rather than merely trends in these values) is not necessarily to be expected, and presumably arises from a fortuitous balancing of the exciton binding energy stabilizing the excited state and strong solvation of the relatively small ions formed on oxidation or reduction. Accordingly, we have examined the frontier molecular orbitals to explain the origin of the unexpected large redshifts observed in the spectra of the azaacenes on halogenation.

The LUMOs of all four compounds are similar in appearance (Fig. 4a), explaining the consistent effect of halogenation. In contrast, the geometric shape of the HOMOs differs between the two classes of molecule; **11a**’/**11b**’ show smaller orbital coefficients on rings 3 and 4 (Fig. 4a), whereas in pair **16a**/**16b** the HOMOs have roughly similar coefficients on all rings. The smaller HOMO coefficients on rings 3 and 4 in **11b**’ lead to its diminished stabilization by the four chlorine substituents when compared with the pair **16a**, in which the HOMO coefficients are larger on these rings (Fig. 4a). The diminished stabilization of the HOMO when going from **11a**’ to **11b**’ is the reason for the induced redshift in the diazaacenes. The same effect is also operative for the larger diazapentacenes **15a** and **15b**, where identical effects are observed according to calculations (**15a**’, **15b**’), electrochemistry and optical spectroscopy (Table 1).

If the proposed explanation is correct, stronger acceptors such as cyano (**16c**) might be anticipated to have a larger effect and reduce

the energy of the optical transitions (and the band gap) further. In such compounds DFT indicates that the HOMO has much smaller coefficients on rings 3 and 4 (Fig. 4b). A disjoint orbital structure¹⁹, that is, spatially separated frontier molecular orbitals results. The disjointing effect is further amplified by electronegative substituents and decreases the transition energies for diazaacenes. When the calculated transition energy for **16c** is compared to that for the parent **11c**’ ($R = H$, $X = CN$), there is a decrease of almost 0.7 eV. This effect is less observed in acenes that have more congruent frontier molecular orbitals¹⁹. When comparing the tetracene **16a** with cyano-substituted **16c**, there also occurs a lowering of the computed transition energy; however, the shift of 0.55 eV is smaller than the effect observed when going from **11a**’ to **11c**’.

The disjoint frontier molecular orbitals in diazaacenes are the defining features and open the door to amplified substituent effects in the engineering of their electronic and optical properties. *N*-Heteroacenes in which optical absorption and electron affinity can be tuned independently are within reach. Some of these materials might prove to be promising electron-transport materials.

In conclusion, we have prepared the hitherto unknown halogenated azaacenes **11b** and **15b**,**c**, which show bathochromically shifted absorptions when compared with their non-halogenated congeners **11a** and the previously unknown **15a**. Bathochromic shift on chlorination is not observed in the acene/tetrachloroacene series, indicating that the pyrazines are a necessary ingredient for this engineering of optical properties. Quantum chemical calculations reveal that this difference in behaviour can be attributed to the substituent-induced disjoint frontier molecular orbitals of the azaacenes. The interplay between pyrazines and electronegative substituents serves as a uniquely useful tool to manipulate the absorption characteristics of *N*-heteroacenes. This effect will enhance the design and tuning of acene-type materials for organic electronics and other applications.

Methods

Synthesis of diazatetracene 11b. 1,2,3,4-Tetrachloro-6,11-bis((triisopropylsilyl)ethynyl)benzo[b]phenazine **11b**. In ethanol (10 ml) and acetic acid (3 ml), **9** (0.200 g, 3.85×10^{-4} mol) and **10b** (0.0950 g, 3.85×10^{-4} mol) were heated to reflux overnight. Aqueous workup, filtration washing with cold methanol (10 ml) and column chromatography (10:1, hexane/dichloromethane) give **11b** as green-black crystals (0.190 g, 67.6%). mp = 179°C (decomp); 1 H-NMR (400 MHz, CDCl₃): δ 8.76 (dd, $^3J = 3.2$ Hz, $^4J = 6.8$ Hz, 2H), 7.70 (dd, $^3J = 3.2$ Hz, $^4J = 6.8$ Hz, 2H), 1.29–1.27 (m, broad, 42H); 13 C-NMR (80 MHz, CDCl₃): δ 140.5, 139.3, 136.6, 134.6, 132.3, 129.0, 127.8, 121.4, 109.7, 101.9, 18.9, 11.6; infrared (KBr): 3,116, 3,062, 2,939, 2,889, 2,862, 2,754, 2,723, 2,360, 2,129, 1,461 cm⁻¹; HRMS (m/z): [M⁺] calcd for C₃₈H₄₆Cl₄N₂Si₂, 726.19537; found 726.19656; analysis (calcd, found for C₃₈H₄₆Cl₄N₂Si₂) C (62.63, 62.60); H (6.36, 6.44).

Synthesis of diazapentacenes 15. 1,4-Bis((triisopropylsilyl)ethynyl)anthracene-2,3-diamine (**13**). To an oven-dried 11 Schlenk flask was added **12** (ref. 2) (5.20 g, 8.71×10^{-3} mol) and dry THF (100 ml). After cooling to 0 °C under N₂, LiAlH₄ (3.31 g, 8.71×10^{-2} mol) was added over 1 h. After 12 h under inert gas, aqueous workup and column chromatography (3:1, hexane/dichloromethane) gave **13** (4.41 g, 89%). mp: stable to 250°C; 1 H-NMR (400 MHz, CDCl₃): δ 8.60 (s, 2H), 7.91 (dd, $^3J = 3.2$, $^4J = 6.4$ Hz, 2H), 7.39 (dd, $^3J = 3.2$, $^4J = 6.4$ Hz, 2H), 4.49 (s, 4H), 1.25 (s, 42H); 13 C-NMR (80 MHz, CDCl₃): δ 139.7, 130.9, 127.8, 127.5, 124.6, 122.8, 102.8, 102.1, 101.7, 18.7, 11.3; infrared (KBr): 3,047, 2,962, 2,862, 2,719, 2,136, 1,932, 1,913, 1,620, 1,550, 1,539 cm⁻¹; HRMS (m/z): [M⁺] calcd for C₃₆H₅₂N₂Si₂, 568.36691; found, 568.36863.

6,13-Bis((triisopropylsilyl)ethynyl)-5,14-dihydronaphtho[2,3-b]phenazine (**14a**). In dichloromethane (50 ml) and acetic acid (3 ml), **13** (0.435 g, 7.65×10^{-4} mol) and **10a**¹ (0.245 g, 2.29×10^{-3} mol) were heated to reflux for 12 h to give **14a** as a metallic red-green solid after aqueous workup and chromatography (hexane) (0.0853 g, 17.5%). mp: 263°C (decomp); 1 H-NMR (400 MHz, CDCl₃): δ 8.169 (s, 2H), 7.75 (dd, $^3J = 3.2$ Hz, $^4J = 6.3$ Hz, 2H), 7.30 (dd, $^3J = 3.2$ Hz, $^4J = 6.4$ Hz, 2H), 6.64 (dd, $^3J = 3.3$ Hz, $^4J = 5.7$ Hz, 2H), 6.33 (dd, $^3J = 3.4$ Hz, $^4J = 5.6$ Hz, 2H), 6.61 (s, 2H), 1.25 (s, 42H); 13 C-NMR (80 MHz, CDCl₃): δ 136.3, 131.6, 129.1, 128.46, 127.7, 124.8, 122.2, 122.1, 113.0, 103.5, 100.9, 96.0, 18.9, 11.4; infrared (KBr): 3,055, 3,028, 2,956, 2,923, 2,864, 2,752, 2,721, 2,360, 2,198, 2,135, 2,030, 1,870, 1,737 cm⁻¹; HRMS (m/z): [M⁺] calcd for C₄₂H₅₄N₂Si₂, 642.3826; found, 642.3849.

6,13-Bis((triisopropylsilyl)ethynyl)naphtho[2,3-b]phenazine (**15a**). In dichloromethane (25 ml) **14a** (0.100 g, 1.56×10^{-4} mol) was stirred for 4 h with an excess of MnO₂; **15a** is obtained after removal of solvent and column chromatography

(3:1, hexane : dichloromethane, green solid 0.0995 g, 99%). mp: 265°C (decomp); $^1\text{H-NMR}$ (400 MHz, CDCl_3): δ 9.41 (s, 2H), 8.16 (dd, $^3J = 3.4\text{ Hz}$, $^4J = 6.9\text{ Hz}$, 2H), 8.02 (dd, $^3J = 3.2\text{ Hz}$, $^4J = 6.6\text{ Hz}$, 2H), 7.75 (dd, $^3J = 3.4\text{ Hz}$, $^4J = 6.9\text{ Hz}$, 2H), 7.46 (dd, $^3J = 3.2\text{ Hz}$, $^4J = 6.6\text{ Hz}$, 2H), 1.36–1.35 (m, broad, 42H); (80 MHz, CDCl_3): δ 145.0, 141.0, 132.9, 132.6, 131.2, 130.5, 128.7, 126.8, 126.8, 120.8, 109.5, 103.8, 19.0, 11.7; infrared (KBr): 3,047, 3,024, 2,956, 2,939, 2,923, 2,862, 2,752, 2,721, 2,136, 2,111, 1,731, 1,600 cm^{-1} ; HRMS (m/z): [M $^+$] calcd for $\text{C}_{42}\text{H}_{52}\text{N}_2\text{Si}_2$: 640.3669 found 640.3674; analysis (calcd, found for $\text{C}_{42}\text{H}_{52}\text{N}_2\text{Si}_2$) C (78.69, 78.11); H (8.18, 8.14).

1,2,3,4-Tetrachloro-6,13-bis((triisopropylsilyl)ethynyl)-5,14-dihydronaphtho[2,3,b]phenazine (**14b**). In ethanol (3 ml) and acetic acid (1.5 ml), **13** (0.200 g, 3.52×10^{-4} mol) and **10b** (0.0864 g, 3.52×10^{-4} mol) were reacted under microwave irradiation (120°C, 10 min). After aqueous workup, **14b** was purified by column chromatography (9:1, hexane/dichloromethane; metallic red-green solid, 0.0631 g, 23%). mp: stable up to 350°C; $^1\text{H-NMR}$ (400 MHz, CDCl_3): δ 8.34 (s, 2H), 7.81 (dd, $^3J = 3.2$, $^4J = 6.4\text{ Hz}$, 2H), 7.39 (dd, $^3J = 3.2$, $^4J = 6.4\text{ Hz}$, 2H), 7.18 (s, 2H), 1.27–1.25 (m, broad, 42H); $^{13}\text{C-NMR}$ (80 MHz, CDCl_3): δ 133.3, 131.9, 128.3, 127.84, 126.9, 125.5, 123.6, 123.2, 114.9, 105.4, 99.5, 99.1, 18.9, 11.4; infrared (KBr): 3,048, 2,927, 2,918, 2,891, 2,863, 2,853, 2,722, 2,554, 2,129, 1,928, 1,888, 1,797, 1,750, 1,579, 1,553, 1,488, cm^{-1} ; HRMS (m/z): [M $^+$] calcd for $\text{C}_{42}\text{H}_{50}\text{N}_2\text{Si}_2\text{Cl}_4$: 778.22667; found, 778.22852.

1,2,3,4-Tetrachloro-6,13-bis((triisopropylsilyl)ethynyl)naphtho[2,3-b]phenazine (**15b**). In dichloromethane (25 ml) **14b** (0.0631 g, 8.08×10^{-5} mol) was stirred for 4 h with an excess of activated MnO_2 ; **15b** was obtained after removal of solvent and column chromatography (3:1, hexane/dichloromethane; dark-green solid, 0.061 g, 99%). mp: 243°C; $^1\text{H-NMR}$ (400 MHz, CDCl_3): δ 9.45 (s, 2H), 8.05 (dd, $^3J = 3.1\text{ Hz}$, $^4J = 6.6\text{ Hz}$, 2H), 7.56 (dd, $^3J = 3.1\text{ Hz}$, $^4J = 6.6\text{ Hz}$, 2H), 1.35–1.33 (m, broad, 42H); $^{13}\text{C-NMR}$ (80 MHz, CDCl_3): δ 139.9, 139.4, 134.6, 133.5, 133.5, 132.3, 128.7, 127.4, 127.2, 121.4, 111.1, 102.9, 19.0, 11.6; infrared (KBr): 3,068, 3,045, 2,953, 2,940, 2,926, 2,920, 2,889, 2,863, 2,756, 2,722, 2,136 cm^{-1} ; HRMS (m/z): [M $^+$] calcd for $\text{C}_{42}\text{H}_{48}\text{N}_2\text{Si}_2\text{Cl}_4$: 776.21102; found, 776.21004; analysis (calcd, found for $\text{C}_{42}\text{H}_{48}\text{N}_2\text{Si}_2\text{Cl}_4$) C (64.77, 64.56); H (6.21, 6.55).

1,2,3,4-Tetrabromo-6,13-bis((triisopropylsilyl)ethynyl)naphtho[2,3-b]phenazine (**14c**). In ethanol (5 ml) and acetic acid (1.5 ml) **13** (0.073 g, 1.28×10^{-4} mol) and **10c** (0.0544 g, 1.28×10^{-4}) were refluxed for 12 h. After aqueous workup, **14c** was purified by column chromatography (hexane; dark red-green solid, 0.0172 g, 14%). mp: 275°C (decomp); $^1\text{H-NMR}$ (400 MHz, CDCl_3): δ 8.30 (s, 2H), 7.75 (dd, $^3J = 3.4\text{ Hz}$, $^4J = 6.4\text{ Hz}$, 2H), 7.34 (dd, $^3J = 3.1\text{ Hz}$, $^4J = 6.4\text{ Hz}$, 2H), 7.27 (s, 2H), 1.23–1.22 (m, broad, 42H); $^{13}\text{C-NMR}$ (80 MHz, CDCl_3): δ 133.8, 131.9, 128.8, 128.5, 127.8, 125.5, 123.2, 118.4, 109.1, 105.4, 99.6, 98.9, 18.9, 11.4; infrared (KBr): 3,045, 2,939, 2,926, 2,920, 2,887, 2,862, 2,721, 2,534, 2,360, 2,143, 2,127, 1,580 cm^{-1} ; HRMS (m/z): [M $^+$] calcd for $\text{C}_{42}\text{H}_{50}\text{N}_2\text{Si}_2\text{Br}_4$: 954.02460; found, 954.02184.

1,2,3,4-Tetrabromo-6,13-bis((triisopropylsilyl)ethynyl)naphtho[2,3-b]phenazine (**15c**). In dichloromethane (25 ml) **14c** (0.0172 g, 1.79×10^{-5}) was stirred for 4 h with an excess of MnO_2 ; **15c** was obtained after solvent removal and column chromatography (3:1, hexane/DCM; dark-green solid; 0.0171 g, 100%). mp: 275°C (decomp); $^1\text{H-NMR}$ (400 MHz, CDCl_3): δ 9.46 (s, 2H), 7.99 (dd, $^3J = 3.2\text{ Hz}$, $^4J = 6.5\text{ Hz}$, 2H), 7.50 (dd, $^3J = 3.2\text{ Hz}$, $^4J = 6.7\text{ Hz}$, 2H), 1.34–1.33 (m, broad, 42H); $^{13}\text{C-NMR}$ (80 MHz, CDCl_3): δ 140.52, 140.48, 133.63, 133.55, 131.7, 129.1, 128.8, 127.45, 127.3, 121.3, 111.1, 103.1, 19.0, 11.7; infrared (KBr): 3,045, 2,954, 2,939, 2,925, 2,889, 2,861, 2,753, 2,722, 2,143, 2,125, 1,531, cm^{-1} ; ESI (m/z): [M $^+$] calcd for $\text{C}_{42}\text{H}_{48}\text{N}_2\text{Si}_2\text{Br}_4$: 952; found, 952. Correct isotopic splitting pattern.

Computational methods. Electronic structure computations were performed at the DFT level using the three-parameter hybrid exchange functional from Becke²⁷ and the correlation functional from Lee *et al.*²⁸ (B3LYP). All computations were carried out with a 6-311 + G*Pople basis set with the Gaussian 2009 program^{28,29}. Geometries of the ground singlet states were completely optimized (RMS gradient 3×10^{-4} , RMS displacement 1.2×10^{-5}). Vertical and adiabatic ionization potentials were computed from the unrestricted B3LYP computations of the corresponding ionic states. Vertical and adiabatic excitation energies were computed within the time-dependent (TD)-DFT approach. The first excited electronic state was completely optimized at the TD-DFT level. The totality of the theoretical characterizations (vertical and adiabatic ionization potentials, electron affinities and excitation energies) along with the B3LYP/6-311 + G*-optimized geometries for the ground state is included as Supplementary Data.

References

- Clar, E. Information on polynuclear aromatic carbohydrates and their derivatives, I. Announcement—dibenzanthracens and their chinones. *Chem. Ber.* **62**, 350–359 (1929).
- Hinsberg, O. Multi-level nitrogenous ring systems. *Liebigs Ann. Chem.* **319**, 257–286 (1901).
- Miao, Q., Nguyen, T. Q., Someya, T., Blanchet, G. B. & Nuckolls, C. Synthesis, assembly, and thin film transistors of dihydroniazapentacene: an isostructural motif for pentacene. *J. Am. Chem. Soc.* **125**, 10284–10287 (2003).
- Anthony, J. E. The larger acenes: versatile organic semiconductors. *Angew. Chem. Int. Ed.* **47**, 452–483 (2008).
- Anthony, J. E. Functionalized acenes and heteroacenes for organic electronics. *Chem. Rev.* **106**, 5028–5048 (2006).
- Coropceanu, V., Malagoli, M., da Silva Filho, D. A., Gruhn, N. E., Bill, T. G. & Brédas, J. L. Hole- and electron-vibrational couplings in oligoacene crystals: intramolecular contributions. *Phys. Rev. Lett.* **89**, 275503 (2002).
- Yoo, S., Domercq, B. & Kippelen, B. Efficient thin-film organic solar cells based on pentacene/C-60 heterojunctions. *Appl. Phys. Lett.* **85**, 5427–5429 (2004).
- Winkler, M. & Houk, K. N. Nitrogen-rich oligoacenes: candidates for *n*-channel organic semiconductors. *J. Am. Chem. Soc.* **129**, 1805–1815 (2007).
- Sakamoto, Y. *et al.* Perfluoropentacene: high-performance p–n junctions and complementary circuits with pentacene. *J. Am. Chem. Soc.* **126**, 8138–8140 (2004).
- Delgado, M. C. R. *et al.* Impact of perfluorination on the charge-transport parameters of oligoacene crystals. *J. Am. Chem. Soc.* **131**, 1502–1512 (2009).
- Chen, Z. H., Muller, P. & Swager, T. M. Syntheses of soluble, pi-stacking tetracene derivatives. *Org. Lett.* **8**, 273–276 (2006).
- Salman, S., Delgado, M. C. R., Coropceanu, V. & Bredas, J. L. Electronic structure and charge-transport parameters of functionalized tetracene crystals: impact of partial fluorination and alkyl or alkoxy derivatization. *Chem. Mater.* **21**, 3593–3601 (2009).
- Miao, S. *et al.* 6,13-Diethynyl-5,7,12,14-tetraazapentacene. *Chem. Eur. J.* **15**, 4990–4993 (2009).
- Bunz, U. H. F. N-Heteroacenes. *Chem. Eur. J.* **15**, 6780–6789 (2009).
- Tang, M. L., Oh, J. H., Reichardt, A. D. & Bao, Z. N. Chlorination: a general route toward electron transport in organic semiconductors. *J. Am. Chem. Soc.* **131**, 3733–3740 (2009).
- Anthony, J. E., Brooks, J. S., Eaton, D. L. & Parkin, S. R. Functionalized pentacene: improved electronic properties from control of solid-state order. *J. Am. Chem. Soc.* **123**, 9482–9483 (2001).
- Pavlovich, V. S. Dispersion interactions, electronic absorption spectra of anthracenes in polar glassy media at 77–300 K and the change in polarizability upon excitation. *J. Appl. Spectroscopy* **74**, 180–187 (2007).
- De Boni, L. *et al.* Two-photon absorption in azoaromatic compounds. *Chem. Phys. Lett.* **361**, 209–213 (2002).
- Zuccheri, A. J., McGrier, P. L. & Bunz, U. H. F. Cross-conjugated cruciform fluorophores. *Acc. Chem. Res.* **43**, 397–408 (2010).
- Acc. Chem. Res. **42**: Thematic Issue 11, Organic Photovoltaics (2009).
- Payne, M. M., Parkin, S. R. & Anthony, J. E. Functionalized higher acenes: hexacene and heptacene. *J. Am. Chem. Soc.* **127**, 8028–8029 (2005).
- Kummer, F. & Zimmermann, H. Electron spectra of linear diazaacenes and tetraazaacenes. *Ber. Bunsenges.* **71**, 1119–1125 (1967).
- Miao, S. *et al.* Are *N,N*-dihydrodiazatetracene derivatives antiaromatic? *J. Am. Chem. Soc.* **130**, 7339–7344 (2008).
- Appleton, A. L. *et al.* Alkynylated aceno[2,1,3]thiadiazoles. *Org. Lett.* **11**, 5222–5225 (2009).
- Wu, J. I., Wannere, C. S., Mo, Y. R., Schleyer, P. V. & Bunz, U. H. F. 4n pi electrons but stable: *N,N*-dihydrodiazapentacenes. *J. Org. Chem.* **74**, 4343–4349 (2009).
- Hansch, C., Leo, A. & Taft, R. W. A survey of Hammett substituent constants and resonance and field parameters. *Chem. Rev.* **91**, 165 (1991).
- Becke, A. D. Density functional thermochemistry. 3. The role of exact exchange. *J. Chem. Phys.* **98**, 5648 (1993).
- Lee, C. T., Yang, W. T. & Parr, R. G. Development of the Colle–Salvetti correlation-energy formula into a functional of the electron-density. *Phys. Rev. B* **37**, 785 (1988).
- Frisch, M. J. *et al.* *Gaussian 09, Revision A.1*, Gaussian, Inc., Wallingford, CT, (2009).
- Bunz, U. H. F. The larger N-heteroacenes. *Pure Appl. Chem.* **82**, 953–968 (2010).

Acknowledgments

The work in the Bunz group was supported by the National Science Foundation (Award CHE-0848833). The work in the Bredas group was primarily supported by the MRSEC Program of the National Science Foundation (Award DMR-0819885). The work in the Marder group was supported by the Office of Naval Research.

Author contributions

U.B. and A.L.A. conceived and designed the experiments; A.L.A. and S.M.B. performed the experiments; J.S.S. performed the calculations; S.B. performed electrochemical measurements. A.L.A., S.B., S.R.M., J.L.B. and U.B. analysed the data, and U.B. wrote the paper. All the authors edited the paper.

Additional information

Supplementary Information accompanies this paper on <http://www.nature.com/naturecommunications>

Competing financial interests: The authors declare no competing financial interests.

Reprints and permission information is available online at <http://npg.nature.com/reprintsandpermissions/>

How to cite this article: Appleton A. L., *et al.* Effects of electronegative substitution on the optical and electronic properties of acenes and diazaacenes. *Nat. Commun.* **1**:91 doi: 10.1038/ncomms1088 (2010).

Erratum

The Article 'Effects of electronegative substitution on the optical and electronic properties of acenes and diazaacenes' (*Nat. Commun.* doi:10.1038/ncomms1088; 2010) was published with the incorrect article number of 90; it should have been 91. This has been corrected as of 22 October 2010.